

On the stability of the low-rank projector-splitting integrator for hyperbolic and parabolic equations

Shiheng Zhang* and Jingwei Hu†

July 22, 2025

Abstract

We study the stability of a class of dynamical low-rank methods—the projector-splitting integrator (PSI)—applied to linear hyperbolic and parabolic equations. Using a von Neumann-type analysis, we investigate the stability of such low-rank time integrator coupled with standard spatial discretizations, including upwind and central finite difference schemes, under two commonly used formulations: discretize-then-project (DtP) and project-then-discretize (PtD). For hyperbolic equations, we show that the stability conditions for DtP and PtD are the same under Lie–Trotter splitting, and that the stability region can be significantly enlarged by using Strang splitting. For parabolic equations, despite the presence of a negative S-step, unconditional stability can still be achieved by employing Crank–Nicolson or a hybrid forward–backward Euler scheme in time stepping. While our analysis focuses on simplified model problems, it offers insight into the stability behavior of PSI for more complex systems, such as those arising in kinetic theory.

Key words. hyperbolic equation, parabolic equation, dynamical low-rank approximation, projector-splitting integrator, finite difference, numerical stability

AMS subject classifications. 35L02, 35K10, 65F55, 65M06, 65M12

1 Introduction

In this work, we are interested in the stability of a class of low-rank integrators applied to hyperbolic and parabolic equations. Our study is primarily motivated by the kinetic Vlasov-Fokker-Planck equation [11], widely used to describe plasma dynamics:

$$\partial_t f + v \cdot \nabla_x f + E(t, x) \cdot \nabla_v f = \nu \nabla_v \cdot (T(t, x) \nabla_v f + (v - u(t, x))f), \quad (1.1)$$

where $f = f(t, x, v)$ is the phase-space distribution function at time $t \geq 0$, position $x \in \Omega \in \mathbb{R}^3$, and velocity $v \in \mathbb{R}^3$. $E(t, x)$ is the electric field, which can be specified externally or determined self-consistently via Poisson’s equation. The right-hand-side of (1.1) is a Fokker-Planck operator describing charged particle collisions, where $T(t, x)$ and $u(t, x)$ denote the temperature and bulk velocity, respectively; these can also be given externally or derived from the moments of f . The parameter ν is the collision frequency, which may range from $\nu \ll 1$ (weak collisions, mildly stiff) to $\nu \gg 1$ (strong collisions, super stiff).

*Department of Applied Mathematics, University of Washington, Seattle, WA 98195 (shzhang3@uw.edu).

†Department of Applied Mathematics, University of Washington, Seattle, WA 98195 (hujw@uw.edu). Corresponding author.

Numerically solving equation (1.1) is computationally expensive, as a method based on a full tensor grid requires $O(N^6)$ complexity, where N is the number of degrees of freedom in each phase-space dimension. To address this, the dynamical low-rank (DLR) method has recently emerged as a powerful on-the-fly dimension reduction technique for solving kinetic equations [5]. The core idea is to decompose the solution f into low-rank factors that depend only on the physical variable x or the velocity variable v , and to evolve these factors in time. This approach reduces the computational complexity to $O(c(r)N^3)$, where $c(r)$ is a prefactor depending on the rank r of the solution.

Among various DLR methods are the projector-splitting integrator (PSI) [10], the augmented BUG integrator [1], the parallel integrator [2], and the recently introduced XL integrator [4]. One of the key differences between PSI and the latter three integrators is that PSI does not require increasing the rank during time evolution and subsequently truncating it at the end of each time step, making it more computationally efficient. Furthermore, since PSI is derived based on operator splitting, it can be formally extended to second order via Strang splitting. In contrast, extending the other integrators to higher-order accuracy in time is relatively difficult.

However, a major issue with PSI is that it involves solving a backward-in-time substep, which can potentially lead to numerical instability and make it less suitable for stiff or dissipative problems. Moreover, there are two possible ways to implement PSI: the discretize-then-project (DtP) approach and the project-then-discretize (PtD) approach. The DtP approach first discretizes the PDE and then applies the low-rank projection to the resulting matrix equation, whereas the PtD approach first performs the low-rank projection and then applies a standard discretization method to the resulting projected PDEs. The PtD approach is more commonly used in the literature (e.g., [6]), as it has been observed that DtP may lead to instability [8]. Nevertheless, there are situations in which DtP is more appropriate, as performing the low-rank projection may result in a non-hyperbolic system that cannot be properly handled by standard discretization methods [3].

Motivated by the two issues discussed above, we systematically study the stability of PSI [10] when applied to hyperbolic and parabolic problems. To simplify the discussion, we consider two prototype equations:

$$\text{hyperbolic: } \partial_t u + a(v)\partial_x u = 0; \quad (1.2)$$

$$\text{parabolic: } \partial_t u = a(v)\partial_{xx} u, \quad a(v) \geq 0. \quad (1.3)$$

Here $u = u(t, x, v)$ is the unknown function, and $a(v)$ denotes the wave speed in the hyperbolic equation and the diffusion coefficient in the parabolic equation (in the latter case, we also assume $a(v) \geq 0$). Equation (1.2) mimics the transport-type operator in (1.1), while equation (1.3) mimics the diffusion-type operator in (1.1). Note that x and v do not carry physical meaning in these prototype problems; x may refer to the velocity variable and v to the physical variable (e.g., $a(v)\partial_{xx}$ can represent the diffusion operator on the right-hand-side of (1.1)).

We first discretize the variable v in equations (1.2) and (1.3), leading to a system of equations. We then study the stability of PSI for the resulting system when coupled with a standard finite difference discretization in x , carried out in either the DtP or PtD framework. Our approach is based on a von Neumann-type analysis, partly inspired by recent work [8]. **Our main findings can be summarized as follows:**

- For the hyperbolic equation (1.2), in both the DtP and PtD approaches, the upwind finite difference method coupled with Lie-Trotter projector-splitting and forward Euler time stepping is stable under a CFL condition of $1/3$, which is more restrictive compared to the CFL condition of 1 for the full tensor method.

- For the parabolic equation (1.3), in both the DtP and PtD approaches, the central finite difference method coupled with Lie-Trotter projector-splitting and Crank-Nicolson time stepping is unconditionally stable. However, when using forward Euler or backward Euler, the scheme is subject to a restrictive CFL condition. To address this, we propose a hybrid-in-time scheme that is unconditionally stable and thus well suited for super stiff problems (i.e., when $a(v) \gg 1$).
- In both cases, we also discuss the stability of PSI when using Strang splitting and a second-order time integrator, which not only improves accuracy but also results in a less restrictive stability condition.

The rest of this paper is organized as follows. In Section 2, we discuss the discretization in the variable v and prepare the system of equations for the subsequent low-rank approximation. We also summarize the spectral properties of certain finite difference matrices relevant in the following discussion. Section 3 is devoted to the stability analysis of the hyperbolic problem, and Section 4 to the parabolic problem. Finally, the paper is concluded in Section 5.

2 Some preliminaries

2.1 Discretization in the v -variable

We first discretize the variable v in equation (1.2), using either a nodal or modal discretization.

In the nodal discretization, we choose the grid points $(v_1, v_2, \dots, v_{N_v})$. The unknown then becomes

$$\mathbf{u}(t, x) = \begin{bmatrix} u(t, x, v_1) \\ \vdots \\ u(t, x, v_{N_v}) \end{bmatrix} \in \mathbb{R}^{N_v},$$

and the equation becomes

$$\partial_t u(t, x, v_i) + a(v_i) \partial_x u(t, x, v_i) = 0, \quad i = 1, \dots, N_v,$$

that is,

$$\partial_t \mathbf{u}(t, x) + A \partial_x \mathbf{u}(t, x) = 0, \tag{2.1}$$

where $A \in \mathbb{R}^{N_v \times N_v}$ is a diagonal matrix with entries $a(v_i)$ on the diagonal.

In the modal discretization, we assume $u(t, x, v) = \sum_{i=1}^{N_v} u_i(t, x) \phi_i(v)$, where $\{\phi_i(v)\}$ is a set of orthonormal basis. The unknown then becomes

$$\mathbf{u}(t, x) = \begin{bmatrix} u_1(t, x) \\ \vdots \\ u_{N_v}(t, x) \end{bmatrix} \in \mathbb{R}^{N_v}. \tag{2.2}$$

Substituting this ansatz into the equation and requiring the residual to be orthogonal to each basis ϕ_i , we obtain

$$\partial_t u_i + \sum_{j=1}^{N_v} \langle a(v) \phi_i(v) \phi_j(v) \rangle_v \partial_x u_j = 0, \quad i = 1, \dots, N_v,$$

where $\langle \cdot \rangle_v$ denotes the integral over the domain of v . This can again be written in the form (2.1), with \mathbf{u} given by (2.2) and the matrix $A \in \mathbb{R}^{N_v \times N_v}$ having entries $(A)_{ij} = \langle a(v) \phi_i(v) \phi_j(v) \rangle_v$.

In both discretizations, the resulting matrix A is a constant symmetric matrix, hence diagonalizable with real eigenvalues:

$$A = R\Lambda R^{-1}, \quad \Lambda = \text{diag}(\lambda_1, \dots, \lambda_{N_v}). \quad (2.3)$$

For such a matrix, we define

$$|A| = R|\Lambda|R^{-1}, \quad |\Lambda| = \text{diag}(|\lambda_1|, \dots, |\lambda_{N_v}|). \quad (2.4)$$

For the parabolic equation (1.3), following the same procedure as above, the discretization in v leads to a system of equations:

$$\partial_t \mathbf{u}(t, x) = A \partial_{xx} \mathbf{u}(t, x), \quad (2.5)$$

where $A \in \mathbb{R}^{N_v \times N_v}$ satisfies the same property as in (2.3). In addition, all eigenvalues $\{\lambda_k\}_{k=1}^{N_v}$ are non-negative due to $a(v) \geq 0$.

2.2 Spectral properties of some useful finite difference matrices

In Sections 3 and 4, we will consider some standard finite difference methods applied to the variable x , such as the upwind and central finite difference schemes. Assuming periodic boundary condition in x , the following two matrices are relevant:

$$M_\alpha = \begin{bmatrix} 0 & 1 & & & -1 \\ -1 & 0 & 1 & & \\ & -1 & 0 & 1 & \\ & & \ddots & \ddots & \ddots \\ & & & -1 & 0 & 1 \\ 1 & & & & -1 & 0 \end{bmatrix} \in \mathbb{R}^{N_x \times N_x}, \quad M_\beta = \begin{bmatrix} -2 & 1 & & & 1 \\ 1 & -2 & 1 & & \\ & 1 & -2 & 1 & \\ & & \ddots & \ddots & \ddots \\ & & & 1 & -2 & 1 \\ 1 & & & & 1 & -2 \end{bmatrix} \in \mathbb{R}^{N_x \times N_x}. \quad (2.6)$$

It can be verified that the matrices M_α and M_β share the same eigenvectors:

$$\mathbf{x}_m = [1, \omega^m, \omega^{2m}, \dots, \omega^{(N_x-1)m}]^T \in \mathbb{C}^{N_x}, \quad \omega = e^{2\pi i/N_x}, \quad m = 0, \dots, N_x - 1, \quad (2.7)$$

with the corresponding eigenvalues:

$$M_\alpha \mathbf{x}_m = \alpha_m \mathbf{x}_m, \quad \alpha_m = 2i \sin\left(\frac{2\pi m}{N_x}\right); \quad M_\beta \mathbf{x}_m = \beta_m \mathbf{x}_m, \quad \beta_m = -2 + 2 \cos\left(\frac{2\pi m}{N_x}\right).$$

To simplify the notation in the following discussion, we introduce

$$\theta_m = \frac{2\pi m}{N_x}, \quad Z_m = \sin \theta_m \in [-1, 1], \quad Y_m = 1 - \cos \theta_m \in [0, 2],$$

then

$$\alpha_m = 2iZ_m, \quad \beta_m = -2Y_m, \quad Z_m^2 = \sin^2 \theta_m = 1 - \cos^2 \theta_m = 1 - (1 - Y_m)^2 = Y_m(2 - Y_m). \quad (2.8)$$

3 Hyperbolic equation

We now consider the DLR approximation for the hyperbolic system (2.1). This can be done in two ways: 1) the DtP approach; 2) the PtD approach. We analyze each of them separately.

3.1 DtP approach

In the DtP approach, we first discretize (2.1) in the x -variable to obtain a matrix differential equation and then apply the low-rank projection/approximation.

Assume a uniform grid $(x_1, x_2, \dots, x_{N_x})$ with spacing Δx and periodic boundary condition. The most natural finite difference method for (2.1) is the upwind scheme [9]:

$$\dot{\mathbf{u}}_j = -\frac{1}{2\Delta x}A(\mathbf{u}_{j+1} - \mathbf{u}_{j-1}) + \frac{1}{2\Delta x}|A|(\mathbf{u}_{j-1} - 2\mathbf{u}_j + \mathbf{u}_{j+1}), \quad j = 1, \dots, N_x, \quad (3.1)$$

where $\mathbf{u}_j(t) = \mathbf{u}(t, x_j)$, and $|A|$ is defined in (2.4).

Define

$$U(t) = \begin{bmatrix} \mathbf{u}_1^T \\ \mathbf{u}_2^T \\ \vdots \\ \mathbf{u}_{N_x}^T \end{bmatrix} \in \mathbb{R}^{N_x \times N_v}, \quad (3.2)$$

and using the matrices M_α and M_β defined in (2.6), the scheme (3.1) (after transpose) can be written as

$$\dot{U} = -\frac{1}{2\Delta x}M_\alpha U A^T + \frac{1}{2\Delta x}M_\beta U |A|^T := F(U). \quad (3.3)$$

This is a $N_x \times N_v$ matrix equation, for which one can apply the standard PSI method [10]. Before analyzing its stability, we first consider a fully discrete scheme for (3.3) using forward Euler time stepping:

$$U^{n+1} = U^n + \Delta t F(U^n). \quad (3.4)$$

We analyze the stability of (3.4) using a von Neumann-type analysis, i.e., examining the Frobenius norm stability of the full solution matrix $\|U^{n+1}\|_F \leq \|U^n\|_F$. This result is well-known, but the technique used here will serve as a baseline for the subsequent low-rank analysis.

Theorem 3.1 (Stability of the Full-Tensor Scheme). *The fully discrete scheme (3.4) for the hyperbolic system (2.1), using the upwind finite difference in space and forward Euler in time, is L^2 -stable if the CFL number satisfies*

$$\nu := \lambda_{\max} \frac{\Delta t}{\Delta x} \leq 1,$$

where $\lambda_{\max} = \max_k |\lambda_k|$ is the largest eigenvalue in magnitude of the matrix A .

Proof. We perform a von Neumann stability analysis by examining the amplification of a single rank-1 mode $\mathbf{x}_m \mathbf{v}_k^T$. Here, $\mathbf{x}_m \in \mathbb{C}^{N_x}$ is a spatial Fourier mode given by (2.7) and an eigenvector of M_α and M_β , with eigenvalues α_m and β_m ; $\mathbf{v}_k \in \mathbb{R}^{N_v}$ is an eigenvector of A and $|A|$, with eigenvalues λ_k and $|\lambda_k|$.

Substituting the mode $U^n = \mathbf{x}_m \mathbf{v}_k^T$ into the scheme (3.4) and using the definition of $F(U)$ in (3.3) gives

$$\begin{aligned} U^{n+1} &= \mathbf{x}_m \mathbf{v}_k^T - \frac{\Delta t}{2\Delta x} M_\alpha (\mathbf{x}_m \mathbf{v}_k^T) A^T + \frac{\Delta t}{2\Delta x} M_\beta (\mathbf{x}_m \mathbf{v}_k^T) |A|^T \\ &= \mathbf{x}_m \mathbf{v}_k^T - \frac{\Delta t}{2\Delta x} (\alpha_m \mathbf{x}_m) (\lambda_k \mathbf{v}_k^T) + \frac{\Delta t}{2\Delta x} (\beta_m \mathbf{x}_m) (|\lambda_k| \mathbf{v}_k^T) \\ &= \left(1 - \frac{\alpha_m \lambda_k \Delta t}{2\Delta x} + \frac{\beta_m |\lambda_k| \Delta t}{2\Delta x} \right) \mathbf{x}_m \mathbf{v}_k^T. \end{aligned}$$

Thus, the amplification factor over one time step is

$$G_{\text{full}}(m, k) = 1 - \frac{\alpha_m \lambda_k \Delta t}{2\Delta x} + \frac{\beta_m |\lambda_k| \Delta t}{2\Delta x} = (1 - |\nu_k| Y_m) - i \nu_k Z_m,$$

where we used the definition of α_m and β_m in (2.8) and the CFL-like number $\nu_k := \lambda_k \frac{\Delta t}{\Delta x}$.

Hence

$$|G_{\text{full}}(m, k)|^2 = (1 - |\nu_k|Y_m)^2 + \nu_k^2 Z_m^2 = 1 + 2Y_m|\nu_k|(|\nu_k| - 1),$$

where we used $Z_m^2 = Y_m(2 - Y_m)$ in the last equality.

For stability, we require $|G_{\text{full}}(m, k)|^2 \leq 1$. Since $Y_m \in [0, 2]$, it can be easily checked that a sufficient condition for the scheme to be stable is $|\nu_k| \leq \nu \leq 1$. \square

We now consider the low-rank approximation for the matrix $U(t)$:

$$U(t) = X(t)S(t)V(t)^T, \quad X \in \mathbb{R}^{N_x \times r}, \quad S \in \mathbb{R}^{r \times r}, \quad V \in \mathbb{R}^{N_v \times r},$$

where r is the rank, and $X^T X = I_r$, $V^T V = I_r$. The PSI method [10] for (3.3) from t^n to t^{n+1} is performed via a sequence of three substeps, if the Lie-Trotter splitting is used. Assuming forward Euler time integration is used in each substep, the scheme reads as follows:

- K-step: Define $K^n = X^n S^n$, and solve for K^{n+1} via

$$K^{n+1} = K^n + \Delta t F(K^n (V^n)^T) V^n. \quad (3.5)$$

Perform QR decomposition $K^{n+1} = X^{n+1} S^{(1)}$ to obtain X^{n+1} and $S^{(1)}$.

- S-step: Solve for $S^{(2)}$ via

$$S^{(2)} = S^{(1)} - \Delta t (X^{n+1})^T F(X^{n+1} S^{(1)} (V^n)^T) V^n. \quad (3.6)$$

- L-step: Define $L^n = S^{(2)} (V^n)^T$, and solve for L^{n+1} via

$$L^{n+1} = L^n + \Delta t (X^{n+1})^T F(X^{n+1} L^n). \quad (3.7)$$

Perform QR decomposition $L^{n+1} = S^{n+1} (V^{n+1})^T$ to obtain S^{n+1} and V^{n+1} .

To analyze the stability of the above scheme, it is convenient to reconstruct the full solution matrix using its low-rank factors. Let $U^n = X^n S^n (V^n)^T$ and $U^{n+1} = X^{n+1} S^{n+1} (V^{n+1})^T$ be the solutions at times t^n and t^{n+1} , and define the intermediate solutions as $U^{(1)} = X^{n+1} S^{(1)} (V^n)^T$ and $U^{(2)} = X^{n+1} S^{(2)} (V^n)^T$. Then the schemes (3.5), (3.6), and (3.7) can be equivalently written as

$$\begin{aligned} U^{(1)} &= U^n + \Delta t F(U^n) V^n (V^n)^T \\ &= U^n - \frac{\Delta t}{2\Delta x} (M_\alpha U^n A^T - M_\beta U^n |A|^T) V^n (V^n)^T, \end{aligned} \quad (3.8)$$

$$\begin{aligned} U^{(2)} &= U^{(1)} - \Delta t X^{n+1} (X^{n+1})^T F(U^{(1)}) V^n (V^n)^T \\ &= U^{(1)} + \frac{\Delta t}{2\Delta x} X^{n+1} (X^{n+1})^T (M_\alpha U^{(1)} A^T - M_\beta U^{(1)} |A|^T) V^n (V^n)^T, \end{aligned} \quad (3.9)$$

$$\begin{aligned} U^{n+1} &= U^{(2)} + \Delta t X^{n+1} (X^{n+1})^T F(U^{(2)}) \\ &= U^{(2)} - \frac{\Delta t}{2\Delta x} X^{n+1} (X^{n+1})^T (M_\alpha U^{(2)} A^T - M_\beta U^{(2)} |A|^T). \end{aligned} \quad (3.10)$$

Here, the definition of $F(U)$ from (3.3) is used in the second line of each equation above. For this combined three-step scheme, we perform a von Neumann analysis similar to that for the full-tensor scheme.

Theorem 3.2 (Stability of the PSI Using the DtP Approach). *The PSI scheme (3.8)-(3.10) for the hyperbolic system (2.1), derived using the DtP approach with the upwind finite difference in space and forward Euler in time, is L^2 -stable if the CFL number satisfies*

$$\nu = \lambda_{\max} \frac{\Delta t}{\Delta x} \leq \frac{1}{3},$$

where $\lambda_{\max} = \max_k |\lambda_k|$ is the largest eigenvalue in magnitude of the matrix A .

Proof. We examine the amplification of a single rank-1 mode $\mathbf{x}_m \mathbf{v}_k^T$, where $\mathbf{x}_m \in \mathbb{C}^{N_x}$ is a spatial Fourier mode given by (2.7) and an eigenvector of M_α and M_β , with eigenvalues α_m and β_m ; $\mathbf{v}_k \in \mathbb{R}^{N_v}$ is an eigenvector of A and $|A|$, with eigenvalues λ_k and $|\lambda_k|$. We further assume \mathbf{v}_k is normalized such that $\mathbf{v}_k^T \mathbf{v}_k = 1$.

We start with $U^n = \mathbf{x}_m \mathbf{v}_k^T$. This implies $X^n S^n = \mathbf{x}_m$, $V^n = \mathbf{v}_k$, and $X^n = \frac{\mathbf{x}_m}{\|\mathbf{x}_m\|}$.

- **Step 1 (equation (3.8)):**

$$\begin{aligned} U^{(1)} &= U^n - \frac{\Delta t}{2\Delta x} (M_\alpha U^n A^T - M_\beta U^n |A|^T) V^n (V^n)^T \\ &= \mathbf{x}_m \mathbf{v}_k^T - \frac{\Delta t}{2\Delta x} (M_\alpha \mathbf{x}_m \mathbf{v}_k^T A^T - M_\beta \mathbf{x}_m \mathbf{v}_k^T |A|^T) \mathbf{v}_k \mathbf{v}_k^T \\ &= \mathbf{x}_m \mathbf{v}_k^T - \frac{\Delta t}{2\Delta x} (\alpha_m \mathbf{x}_m \lambda_k \mathbf{v}_k^T - \beta_m \mathbf{x}_m |\lambda_k| \mathbf{v}_k^T) \mathbf{v}_k \mathbf{v}_k^T. \end{aligned}$$

Since $\mathbf{v}_k^T \mathbf{v}_k = 1$, we have

$$U^{(1)} = \left(1 - \frac{\alpha_m \lambda_k \Delta t}{2\Delta x} + \frac{\beta_m |\lambda_k| \Delta t}{2\Delta x} \right) \mathbf{x}_m \mathbf{v}_k^T := P_1(m, k) \mathbf{x}_m \mathbf{v}_k^T.$$

This implies $X^{n+1} S^{(1)} = P_1(m, k) \mathbf{x}_m$, and $X^{n+1} = \frac{\mathbf{x}_m}{\|\mathbf{x}_m\|}$.

- **Step 2 (equation (3.9)):**

$$\begin{aligned} U^{(2)} &= U^{(1)} + \frac{\Delta t}{2\Delta x} X^{n+1} (X^{n+1})^T (M_\alpha U^{(1)} A^T - M_\beta U^{(1)} |A|^T) V^n (V^n)^T \\ &= P_1(m, k) \mathbf{x}_m \mathbf{v}_k^T + \frac{\Delta t}{2\Delta x} \frac{\mathbf{x}_m \mathbf{x}_m^T}{\|\mathbf{x}_m\|^2} (\alpha_m P_1(m, k) \mathbf{x}_m \lambda_k \mathbf{v}_k^T - \beta_m P_1(m, k) \mathbf{x}_m |\lambda_k| \mathbf{v}_k^T) \mathbf{v}_k \mathbf{v}_k^T \\ &= P_1(m, k) \mathbf{x}_m \mathbf{v}_k^T + \frac{\Delta t}{2\Delta x} (\alpha_m P_1(m, k) \lambda_k - \beta_m P_1(m, k) |\lambda_k|) \mathbf{x}_m \mathbf{v}_k^T \\ &= P_1(m, k) \left(1 + \frac{\alpha_m \lambda_k \Delta t}{2\Delta x} - \frac{\beta_m |\lambda_k| \Delta t}{2\Delta x} \right) \mathbf{x}_m \mathbf{v}_k^T \\ &= P_1(m, k) (2 - P_1(m, k)) \mathbf{x}_m \mathbf{v}_k^T. \end{aligned}$$

Define $P_2(m, k) = 2 - P_1(m, k)$, then $U^{(2)} = P_1(m, k) P_2(m, k) \mathbf{x}_m \mathbf{v}_k^T$.

- **Step 3 (equation (3.10)):**

$$\begin{aligned} U^{n+1} &= U^{(2)} - \frac{\Delta t}{2\Delta x} X^{n+1} (X^{n+1})^T (M_\alpha U^{(2)} A^T - M_\beta U^{(2)} |A|^T) \\ &= P_1(m, k) P_2(m, k) \mathbf{x}_m \mathbf{v}_k^T - \frac{\Delta t}{2\Delta x} \frac{\mathbf{x}_m \mathbf{x}_m^T}{\|\mathbf{x}_m\|^2} (\alpha_m P_1(m, k) P_2(m, k) \mathbf{x}_m \lambda_k \mathbf{v}_k^T - \beta_m P_1(m, k) P_2(m, k) \mathbf{x}_m |\lambda_k| \mathbf{v}_k^T) \\ &= P_1(m, k) P_2(m, k) \mathbf{x}_m \mathbf{v}_k^T - \frac{\Delta t}{2\Delta x} \mathbf{x}_m (\alpha_m P_1(m, k) P_2(m, k) \lambda_k \mathbf{v}_k^T - \beta_m P_1(m, k) P_2(m, k) |\lambda_k| \mathbf{v}_k^T) \\ &= P_1(m, k) P_2(m, k) \left(1 - \frac{\alpha_m \lambda_k \Delta t}{2\Delta x} + \frac{\beta_m |\lambda_k| \Delta t}{2\Delta x} \right) \mathbf{x}_m \mathbf{v}_k^T \\ &= P_1^2(m, k) P_2(m, k) \mathbf{x}_m \mathbf{v}_k^T. \end{aligned}$$

This implies $X^{n+1}S^{n+1} = P_1^2(m, k)P_2(m, k)\mathbf{x}_m$, and $V^{n+1} = \mathbf{v}_k$.

Therefore, the total amplification factor over one time step for the mode $U^n = \mathbf{x}_m \mathbf{v}_k^T$ is

$$G_{\text{DtP}}(m, k) = P_1(m, k)^2 P_2(m, k).$$

Note that $P_1(m, k)$ is the same as the amplification factor $G_{\text{full}}(m, k)$ of the full-tensor scheme.

Using the definition of α_m and β_m in (2.8) and the CFL-like number $\nu_k = \lambda_k \frac{\Delta t}{\Delta x}$, we have

$$P_1(m, k) = (1 - |\nu_k|Y_m) - i\nu_k Z_m, \quad (3.11)$$

$$P_2(m, k) = 2 - P_1(m, k) = (1 + |\nu_k|Y_m) + i\nu_k Z_m. \quad (3.12)$$

Hence

$$|P_1(m, k)|^2 = (1 - |\nu_k|Y_m)^2 + \nu_k^2 Z_m^2 = 1 + 2Y_m |\nu_k| (|\nu_k| - 1), \quad (3.13)$$

$$|P_2(m, k)|^2 = (1 + |\nu_k|Y_m)^2 + \nu_k^2 Z_m^2 = 1 + 2Y_m |\nu_k| (|\nu_k| + 1),$$

where we used $Z_m^2 = Y_m(2 - Y_m)$. Therefore,

$$\begin{aligned} |G_{\text{DtP}}(m, k)|^2 &= |P_1(m, k)|^2 |P_2(m, k)|^2 = |P_1(m, k)|^4 |P_2(m, k)|^2 \\ &= [1 + 2Y_m |\nu_k| (|\nu_k| - 1)]^2 [1 + 2Y_m |\nu_k| (|\nu_k| + 1)] := h(Y_m, |\nu_k|). \end{aligned}$$

For stability, we require $|G_{\text{DtP}}(m, k)|^2 \leq 1$. In the following, we will show that this is satisfied for all $Y_m \in [0, 2]$ if $|\nu_k| \leq \nu \leq 1/3$.

Denote $|\nu_k| = \mu$. Taking the derivative of h w.r.t. Y_m gives

$$\frac{\partial h}{\partial Y_m} = 2 \underbrace{\mu}_{\geq 0} \underbrace{[1 + 2Y_m \mu (\mu - 1)]}_{\geq 0, \text{ since (3.13)}} \underbrace{[3\mu - 1 + 6Y_m \mu (\mu^2 - 1)]}_{\leq 0, \text{ if } \mu \leq \frac{1}{3}}.$$

Therefore,

$$\frac{\partial h}{\partial Y_m} \leq 0 \quad \text{for all } Y_m \in [0, 2], \quad \text{if } \mu \in [0, 1/3].$$

So $h(Y_m, \mu)$ is a non-increasing function of Y_m on the interval $[0, 2]$, whose maximum value occurs at $Y_m = 0$: $h(0, \mu) = 1$. Conversely, if $\mu > 1/3$, the term $(3\mu - 1)$ is positive, making the derivative $\frac{\partial h}{\partial Y_m}$ positive at $Y_m = 0$. This causes $h(Y_m, \mu)$ to increase above value 1 for small positive Y_m , leading to instability. Figure 1 is a contour plot of $h(Y_m, \mu)$, from which it is easy to see that $\mu \leq 1/3$ is a sufficient condition to guarantee stability. \square

Remark 3.1. *The previous analysis can be easily extended to the PSI method based on Strang splitting. Assume it is implemented as a half K-step, half S-step, full L-step, half S-step, and half K-step, and a second-order strong-stability-preserving Runge-Kutta (SSP-RK2) scheme [7] is used in each substep:*

$$\begin{aligned} U^{(1)} &= U^n + \Delta t F(U^n), \\ U^{(2)} &= U^{(1)} + \Delta t F(U^{(1)}), \\ U^{n+1} &= \frac{1}{2}(U^n + U^{(2)}). \end{aligned}$$

The amplification factor for this scheme over Δt step is

$$\bar{P}_1(m, k; \Delta t) = \frac{1}{2}(1 + P_1^2(m, k)).$$

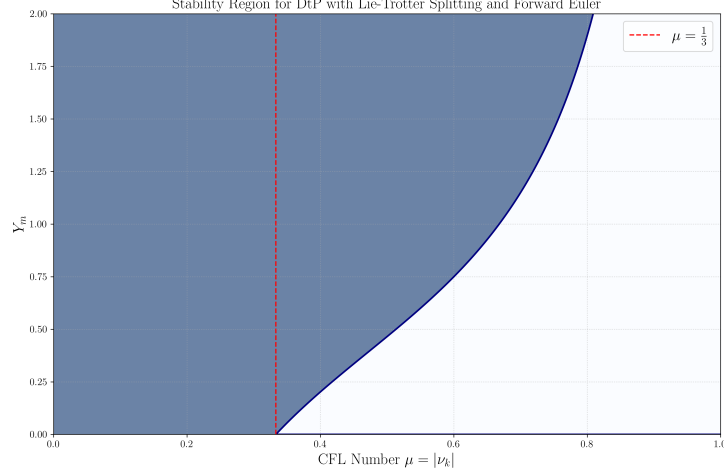


Figure 1: Contour plot of $|G_{\text{DtP}}(m, k)|^2 = h(Y_m, \mu)$. The shaded region corresponds to where $h(Y_m, \mu) \leq 1$. Therefore, $\mu \leq 1/3$ is a sufficient condition to guarantee stability.

Using the definition of $P_1(m, k)$ in (3.11), we obtain

$$|\bar{P}_1(m, k; \Delta t)|^2 = \frac{1}{4} [1 + (1 - |\nu_k|Y_m)^2 - \nu_k^2 Y_m(2 - Y_m)]^2 + (1 - |\nu_k|Y_m)^2 \nu_k^2 Y_m(2 - Y_m). \quad (3.14)$$

If performing SSP-RK2 backward in time, the amplification factor over Δt step is

$$\bar{P}_2(m, k; \Delta t) = \frac{1}{2}(1 + P_2^2(m, k)).$$

Using the definition of $P_2(m, k)$ in (3.12), we obtain

$$|\bar{P}_2(m, k; \Delta t)|^2 = \frac{1}{4} [1 + (1 + |\nu_k|Y_m)^2 - \nu_k^2 Y_m(2 - Y_m)]^2 + (1 + |\nu_k|Y_m)^2 \nu_k^2 Y_m(2 - Y_m). \quad (3.15)$$

Therefore, the total amplification factor for the PSI with Strang splitting and SSP-RK2 is given by

$$G_{\text{DtP-Strang-RK2}}(m, k) = \bar{P}_1(m, k; \Delta t/2) \cdot \bar{P}_2(m, k; \Delta t/2) \cdot \bar{P}_1(m, k; \Delta t) \cdot \bar{P}_2(m, k; \Delta t/2) \cdot \bar{P}_1(m, k; \Delta t/2),$$

and

$$|G_{\text{DtP-Strang-RK2}}(m, k)|^2 = |\bar{P}_1(m, k; \Delta t/2)|^4 |\bar{P}_2(m, k; \Delta t/2)|^4 |\bar{P}_1(m, k; \Delta t)|^2.$$

Here, $|\bar{P}_1(m, k; \Delta t)|^2$ and $|\bar{P}_2(m, k; \Delta t)|^2$ are given by (3.14) and (3.15). The formulas for $\Delta t/2$ are obtained by replacing ν_k with $\nu_k/2$.

A contour plot of $|G_{\text{DtP-Strang-RK2}}(m, k)|^2$ is shown in Figure 2. Interestingly, the stability region is much larger than that of the first-order scheme.

3.2 PtD approach

In the PtD approach, we first apply the low-rank projection/approximation to the hyperbolic system (2.1), obtaining three equations (the K, S, and L Steps), and then discretize each equation in the x -variable.

It is convenient to use the transposed version of (2.1):

$$\partial_t \mathbf{u}^T(t, x) = -\partial_x \mathbf{u}^T(t, x) A^T, \quad \mathbf{u} \in \mathbb{R}^{N_v}, \quad (3.16)$$

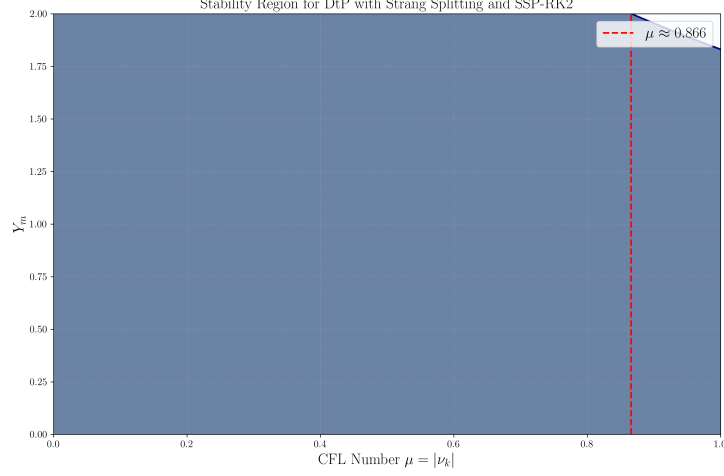


Figure 2: Contour plot of $|G_{\text{DtP-Strang-RK2}}(m, k)|^2 = h(Y_m, \mu)$. The shaded region corresponds to where $h(Y_m, \mu) \leq 1$. Therefore, $\mu \leq 0.866$ is a sufficient condition to guarantee stability.

and to consider the low-rank approximation:

$$\mathbf{u}^T(t, x) = \mathbf{x}^T(t, x)S(t)V(t)^T, \quad \mathbf{x} \in \mathbb{R}^r, \quad S \in \mathbb{R}^{r \times r}, \quad V \in \mathbb{R}^{N_v \times r}.$$

Here, r is the rank, $\langle \mathbf{x}\mathbf{x}^T \rangle_x = I_r$, where $\langle \cdot \rangle_x$ denotes the integral over the domain of x , and $V^T V = I_r$. The projected equations for (3.16) using PSI are:

- K-step: $\mathbf{k}^T(t, x) = \mathbf{x}^T(t, x)S(t)$,

$$\partial_t \mathbf{k}^T = -\partial_x \mathbf{k}^T \tilde{A}^T, \quad \tilde{A} := V^T A V \in \mathbb{R}^{r \times r}. \quad (3.17)$$

Since A is symmetric, \tilde{A} is symmetric and hence diagonalizable. Then $|\tilde{A}|$ can be defined similarly as in (2.4). We discretize (3.17) in x using the upwind scheme. Assume a uniform grid (x_1, \dots, x_{N_x}) with spacing Δx and periodic boundary condition. Let $\mathbf{x}_j(t) = \mathbf{x}(t, x_j)$ and $\mathbf{k}_j^T(t) = \mathbf{x}_j^T(t)S(t)$. We have

$$\dot{\mathbf{k}}_j^T = -\frac{1}{2\Delta x}(\mathbf{k}_{j+1}^T - \mathbf{k}_{j-1}^T)\tilde{A}^T + \frac{1}{2\Delta x}(\mathbf{k}_{j-1}^T - 2\mathbf{k}_j^T + \mathbf{k}_{j+1}^T)|\tilde{A}|^T. \quad (3.18)$$

Introduce:

$$X(t) = \sqrt{\Delta x} \begin{bmatrix} \mathbf{x}_1^T \\ \mathbf{x}_2^T \\ \vdots \\ \mathbf{x}_{N_x}^T \end{bmatrix} \in \mathbb{R}^{N_x \times r}, \quad K(t) = X(t)S(t),$$

then $X^T X = I_r$, and (3.18) can be written as

$$\dot{K} = -\frac{1}{2\Delta x}M_\alpha K \tilde{A}^T + \frac{1}{2\Delta x}M_\beta K |\tilde{A}|^T, \quad (3.19)$$

where M_α and M_β are given by (2.6).

- S-step:

$$\dot{S} = \langle \mathbf{x} \partial_x \mathbf{x}^T \rangle_x S \tilde{A}^T.$$

After discretizing in x using central finite difference, this becomes

$$\dot{S} = \frac{1}{2\Delta x} X^T M_\alpha X S \tilde{A}^T. \quad (3.20)$$

- L-step: $L(t) = S(t)V(t)^T$,

$$\dot{L} = -\langle \mathbf{x} \partial_x \mathbf{x}^T \rangle_x L A^T.$$

After discretizing in x using central finite difference, this becomes

$$\dot{L} = -\frac{1}{2\Delta x} X^T M_\alpha X L A^T. \quad (3.21)$$

If the forward Euler time stepping is used in each substep, the schemes (3.19), (3.20), and (3.21) can be equivalently written as

$$U^{(1)} = U^n - \frac{\Delta t}{2\Delta x} \left(M_\alpha (U^n V^n) \tilde{A}^T - M_\beta (U^n V^n) |\tilde{A}|^T \right) (V^n)^T, \quad (3.22)$$

$$U^{(2)} = U^{(1)} + \frac{\Delta t}{2\Delta x} X^{n+1} (X^{n+1})^T M_\alpha (U^{(1)} V^n) \tilde{A}^T (V^n)^T, \quad (3.23)$$

$$U^{n+1} = U^{(2)} - \frac{\Delta t}{2\Delta x} X^{n+1} (X^{n+1})^T (M_\alpha U^{(2)} A^T), \quad (3.24)$$

where $\tilde{A} = (V^n)^T A V^n$, and the solutions U^n , $U^{(1)}$, $U^{(2)}$, U^{n+1} are defined the same as in the previous subsection.

We perform a similar von Neumann analysis as in the previous subsection. Interestingly, the resulting CFL condition in the PtD approach appears to be the same as that in the DtP approach.

Theorem 3.3 (Stability of the PSI Using the PtD Approach). *The PSI scheme (3.22)-(3.24) for the hyperbolic system (2.1), derived using the PtD approach with the upwind finite difference in K-step, central finite difference in S- and L-steps, and forward Euler in time, is L^2 -stable if the CFL number satisfies*

$$\nu = \lambda_{\max} \frac{\Delta t}{\Delta x} \leq \frac{1}{3},$$

where $\lambda_{\max} = \max_k |\lambda_k|$ is the largest eigenvalue in magnitude of the matrix A .

Proof. We examine the amplification of a single rank-1 mode $U^n = \mathbf{x}_m \mathbf{v}_k^T$, where $\mathbf{x}_m \in \mathbb{C}^{N_x}$ is a spatial Fourier mode given by (2.7) and an eigenvector of M_α and M_β , with eigenvalues α_m and β_m ; $\mathbf{v}_k \in \mathbb{R}^{N_v}$ is an eigenvector of A and $|A|$, with eigenvalues λ_k and $|\lambda_k|$. We further assume \mathbf{v}_k is normalized such that $\mathbf{v}_k^T \mathbf{v}_k = 1$. This implies $X^n S^n = \mathbf{x}_m$, $V^n = \mathbf{v}_k$. Hence $\tilde{A} = (V^n)^T A V^n = \mathbf{v}_k^T A \mathbf{v}_k = \mathbf{v}_k^T (\lambda_k \mathbf{v}_k) = \lambda_k$, and $|\tilde{A}| = |\lambda_k|$.

- **Step 1 (equation (3.22)):** With $U^n V^n = \mathbf{x}_m \mathbf{v}_k^T \mathbf{v}_k = \mathbf{x}_m$, we have

$$\begin{aligned} U^{(1)} &= U^n - \frac{\Delta t}{2\Delta x} (M_\alpha \mathbf{x}_m \tilde{A}^T - M_\beta \mathbf{x}_m |\tilde{A}|^T) \mathbf{v}_k^T \\ &= \mathbf{x}_m \mathbf{v}_k^T - \frac{\Delta t}{2\Delta x} ((\alpha_m \mathbf{x}_m) \lambda_k - (\beta_m \mathbf{x}_m) |\lambda_k|) \mathbf{v}_k^T \\ &= \left(1 - \frac{\alpha_m \lambda_k \Delta t}{2\Delta x} + \frac{\beta_m |\lambda_k| \Delta t}{2\Delta x} \right) \mathbf{x}_m \mathbf{v}_k^T := P_1(m, k) \mathbf{x}_m \mathbf{v}_k^T. \end{aligned}$$

This implies $X^{n+1} = \frac{\mathbf{x}_m}{\|\mathbf{x}_m\|}$.

- **Step 2 (equation (3.23)):** With $U^{(1)} V^n = P_1(m, k) \mathbf{x}_m$, we have

$$\begin{aligned} U^{(2)} &= U^{(1)} + \frac{\Delta t \mathbf{x}_m \mathbf{x}_m^T}{2\Delta x \|\mathbf{x}_m\|^2} M_\alpha (P_1(m, k) \mathbf{x}_m) \tilde{A}^T \mathbf{v}_k^T \\ &= P_1(m, k) \left(1 + \frac{\alpha_m \lambda_k \Delta t}{2\Delta x} \right) \mathbf{x}_m \mathbf{v}_k^T. \end{aligned}$$

Define $P_2(m, k) = 1 + \frac{\alpha_m \lambda_k \Delta t}{2\Delta x}$. Then $U^{(2)} = P_1(m, k) P_2(m, k) \mathbf{x}_m \mathbf{v}_k^T$.

- **Step 3 (equation (3.24)):** With $U^{(2)} = P_1(m, k)P_2(m, k)\mathbf{x}_m\mathbf{v}_k^T$, we have

$$\begin{aligned}
U^{n+1} &= U^{(2)} - \frac{\Delta t \mathbf{x}_m \mathbf{x}_m^T}{2\Delta x \|\mathbf{x}_m\|^2} (M_\alpha P_1(m, k)P_2(m, k)\mathbf{x}_m\mathbf{v}_k^T A^T) \\
&= U^{(2)} - \frac{\Delta t}{2\Delta x} \frac{\mathbf{x}_m \mathbf{x}_m^T}{\|\mathbf{x}_m\|^2} (\alpha_m P_1(m, k)P_2(m, k)\mathbf{x}_m \lambda_k \mathbf{v}_k^T) \\
&= P_1(m, k)P_2(m, k) \left(1 - \frac{\alpha_m \lambda_k \Delta t}{2\Delta x} \right) \mathbf{x}_m \mathbf{v}_k^T.
\end{aligned}$$

Define $P_3(m, k) = 2 - P_2(m, k)$. Then $U^{n+1} = P_1(m, k)P_2(m, k)P_3(m, k)\mathbf{x}_m\mathbf{v}_k^T$.

Therefore, the total amplification factor over one time step for the mode $U^n = \mathbf{x}_m\mathbf{v}_k^T$ is

$$G_{\text{PtD}}(m, k) = P_1(m, k)P_2(m, k)P_3(m, k).$$

Note again that $P_1(m, k)$ is the same as the amplification factor $G_{\text{full}}(m, k)$ of the full-tensor scheme.

Using the definition of α_m and β_m in (2.8) and the CFL-like number $\nu_k = \lambda_k \frac{\Delta t}{\Delta x}$, we have

$$P_1(m, k) = (1 - |\nu_k|Y_m) - i\nu_k Z_m, \quad (3.25)$$

$$P_2(m, k) = 1 + i\nu_k Z_m, \quad (3.26)$$

$$P_3(m, k) = 1 - i\nu_k Z_m. \quad (3.27)$$

Hence

$$\begin{aligned}
|P_1(m, k)|^2 &= (1 - |\nu_k|Y_m)^2 + \nu_k^2 Z_m^2 = 1 + 2Y_m |\nu_k| (|\nu_k| - 1), \\
P_2(m, k)P_3(m, k) &= 1 + \nu_k^2 Z_m^2 = 1 + \nu_k^2 Y_m (2 - Y_m),
\end{aligned}$$

where we used $Z_m^2 = Y_m(2 - Y_m)$. Therefore,

$$\begin{aligned}
|G_{\text{PtD}}(m, k)|^2 &= |P_1(m, k)|^2 |P_2(m, k)P_3(m, k)|^2 \\
&= [1 + 2Y_m |\nu_k| (|\nu_k| - 1)] [1 + \nu_k^2 Y_m (2 - Y_m)]^2 := h(Y_m, |\nu_k|).
\end{aligned}$$

For stability, we require $|G_{\text{PtD}}(m, k)|^2 \leq 1$. In the following, we will show that this is satisfied for all $Y_m \in [0, 2]$ if $|\nu_k| \leq \nu \leq 1/3$.

Denote $|\nu_k| = \mu$. Taking the derivative of h w.r.t. Y_m gives

$$\frac{\partial h}{\partial Y_m} = 2 \underbrace{\mu}_{\geq 0} \underbrace{[1 + \mu^2 Y_m (2 - Y_m)]}_{\geq 0, \text{ since } Y_m(2 - Y_m) = Z_m^2} \underbrace{[(3\mu - 1) + 2\mu(3\mu^2 - 3\mu - 1)Y_m + 5\mu^2(1 - \mu)Y_m^2]}_{:=g(Y_m), \text{ a parabola}}.$$

For the parabola $g(Y_m)$, if $\mu \in [0, 1/3]$, it opens upward. Moreover, it can be checked that $g(0) \leq 0$ and $g(2) \leq 0$. Hence $g(Y_m) \leq 0$ for all $Y_m \in [0, 2]$. Therefore,

$$\frac{\partial h}{\partial Y_m} \leq 0 \quad \text{for all } Y_m \in [0, 2], \quad \text{if } \mu \in [0, 1/3].$$

So $h(Y_m, \mu)$ is a non-increasing function of Y_m on the interval $[0, 2]$, whose maximum value occurs at $Y_m = 0$: $h(0, \mu) = 1$. Similar to the proof in Theorem 3.2, since the derivative $\frac{\partial h}{\partial Y_m}$ at $Y_m = 0$ is positive for any $\mu > 1/3$, $h(Y_m, \mu)$ increases above 1 for small positive Y_m , leading to instability. Figure 3 is a contour plot of $h(Y_m, \mu)$, from which it is easy to see that $\mu \leq 1/3$ is a sufficient condition to guarantee stability. \square

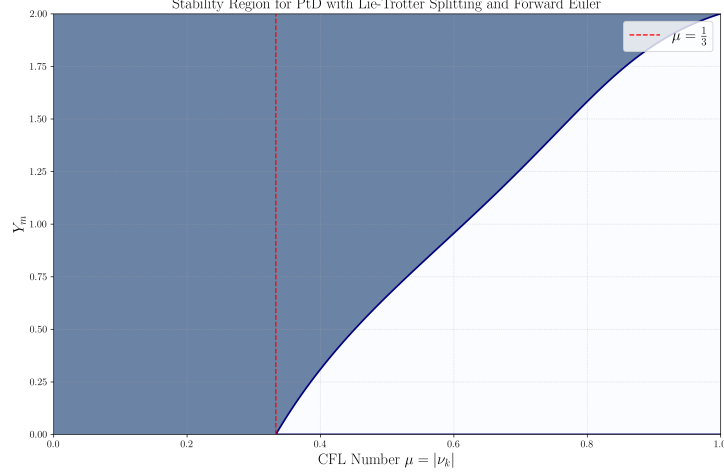


Figure 3: Contour plot of $|G_{\text{PtD}}(m, k)|^2 = h(Y_m, \mu)$; The shaded region corresponds to where $h(Y_m, \mu) \leq 1$. Therefore, $\mu \leq 1/3$ is a sufficient condition to guarantee stability.

Remark 3.2. We note that the amplification factors in the DtP and PtD approaches are different. This is because the upwind scheme is used throughout in the DtP approach, whereas in the PtD approach, upwind is only used in the K-step, and the central finite difference is used in the S-step and L-step. The fact that both approaches yield the same stability region, $\nu \leq 1/3$, is a non-trivial coincidence, resulting from the two different amplification functions sharing identical first-order behavior near the zero-frequency mode (compare Figure 1 and Figure 3).

Remark 3.3. It is worth noting that the PtD approach allows for flexibility in the discretization of each substep (here we have simply used the most natural finite difference scheme for each one). This flexibility can be leveraged to improve the overall stability of the scheme. For instance, as demonstrated in [8], adding a specific stabilization term to the S-step can relax the time-step restriction, increasing the CFL number constraint to 1.

Remark 3.4. Similarly to Remark 3.1, we can analyze the stability of PSI based on Strang splitting and SSP-RK2 scheme used in each substep. We have

$$G_{\text{PtD-Strang-RK2}}(m, k) = \bar{P}_1(m, k; \Delta t/2) \cdot \bar{P}_2(m, k; \Delta t/2) \cdot \bar{P}_3(m, k; \Delta t) \cdot \bar{P}_2(m, k; \Delta t/2) \cdot \bar{P}_1(m, k; \Delta t/2),$$

and

$$|G_{\text{PtD-Strang-RK2}}(m, k)|^2 = |\bar{P}_1(m, k; \Delta t/2)|^4 |\bar{P}_2(m, k; \Delta t/2)|^4 |\bar{P}_3(m, k; \Delta t)|^2.$$

Here,

$$\bar{P}_1(m, k; \Delta t) = \frac{1}{2}(1 + P_1^2(m, k)), \quad \bar{P}_2(m, k; \Delta t) = \frac{1}{2}(1 + P_2^2(m, k)), \quad \bar{P}_3(m, k; \Delta t) = \frac{1}{2}(1 + P_3^2(m, k)).$$

Using the definition of $P_1(m, k)$, $P_2(m, k)$, $P_3(m, k)$ in (3.25)-(3.27), we find that

$$\begin{aligned} |\bar{P}_1(m, k; \Delta t)|^2 &= \frac{1}{4} [1 + (1 - |\nu_k| Y_m)^2 - \nu_k^2 Y_m (2 - Y_m)]^2 + (1 - |\nu_k| Y_m)^2 \nu_k^2 Y_m (2 - Y_m), \\ |\bar{P}_2(m, k; \Delta t)|^2 &= |\bar{P}_3(m, k; \Delta t)|^2 = \frac{1}{4} [2 - \nu_k^2 Y_m (2 - Y_m)]^2 + \nu_k^2 Y_m (2 - Y_m). \end{aligned}$$

The formulas for $\Delta t/2$ are obtained by replacing ν_k with $\nu_k/2$.

A contour plot of $|G_{\text{PtD-Strang-RK2}}(m, k)|^2$ is shown in Figure 4, where the stability region is significantly larger than that of the first-order scheme. This suggests that, in practice, the PtD approach combined with Strang splitting and second-order time integrator is preferred due to its better stability and accuracy.

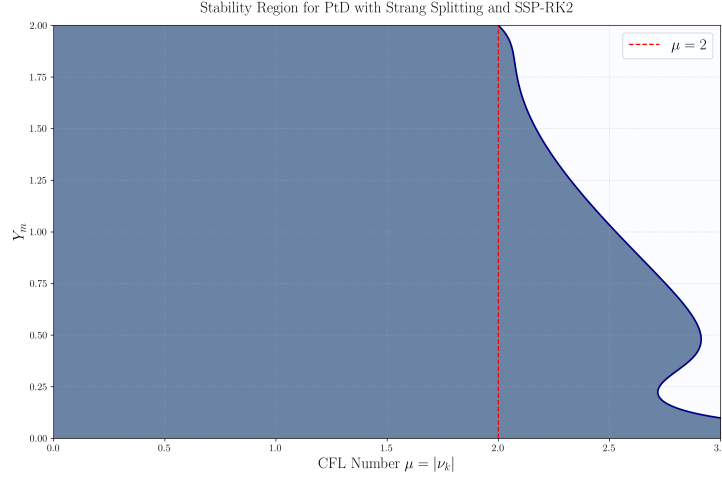


Figure 4: Contour plot of $|G_{\text{PtD-Strang-RK2}}(m, k)|^2 = h(Y_m, \mu)$. The shaded region corresponds to where $h(Y_m, \mu) \leq 1$. Therefore, $\mu \leq 2$ is a sufficient condition to guarantee stability.

4 Parabolic equation

For the parabolic system (2.5), we proceed as before to analyze both the DtP and PtD approaches.

4.1 DtP approach

In the DtP approach, we first discretize (2.5) in x using the standard second-order central difference scheme:

$$\dot{\mathbf{u}}_j = \frac{1}{(\Delta x)^2} A(\mathbf{u}_{j-1} - 2\mathbf{u}_j + \mathbf{u}_{j+1}), \quad j = 1, \dots, N_x.$$

Using the same notation $U(t) \in \mathbb{R}^{N_x \times N_v}$ defined in (3.2) and the matrix M_β given in (2.6), this can be written as:

$$\dot{U} = \frac{1}{(\Delta x)^2} M_\beta U A^T := Q(U). \quad (4.1)$$

We first consider a full-tensor scheme by applying the θ -scheme to (4.1):

$$\frac{U^{n+1} - U^n}{\Delta t} = (1 - \theta)Q(U^n) + \theta Q(U^{n+1}), \quad (4.2)$$

where $\theta = 0$ corresponds to forward Euler, $\theta = 1$ to backward Euler, and $\theta = 1/2$ to Crank-Nicolson.

Theorem 4.1 (Stability of the Full-Tensor Scheme). *The fully discrete scheme (4.2) for the parabolic system (2.5), using the central finite difference in space and θ -scheme in time, has the following stability properties. Define the CFL number as*

$$\nu := \lambda_{\max} \frac{\Delta t}{(\Delta x)^2},$$

where $\lambda_{\max} = \max_k \lambda_k$ is the largest eigenvalue of the matrix A (recall that all eigenvalues of A are non-negative).

- If $\theta \in [1/2, 1]$, the scheme is unconditionally stable. This includes backward Euler ($\theta = 1$) and Crank-Nicolson ($\theta = 1/2$).
- If $\theta \in [0, 1/2)$, the scheme is stable provided $\nu \leq \frac{1}{2(1-2\theta)}$. For forward Euler ($\theta = 0$), this condition reduces to $\nu \leq 1/2$.

Proof. We examine the amplification of a single rank-1 mode $\mathbf{x}_m \mathbf{v}_k^T$, where $\mathbf{x}_m \in \mathbb{C}^{N_x}$ is a spatial Fourier mode given by (2.7) and an eigenvector of M_β with eigenvalue β_m ; $\mathbf{v}_k \in \mathbb{R}^{N_v}$ is an eigenvector of A with eigenvalue λ_k .

We first rewrite the scheme (4.2) as:

$$U^{n+1} - \theta \Delta t Q(U^{n+1}) = U^n + (1 - \theta) \Delta t Q(U^n).$$

We assume $U^n = \mathbf{x}_m \mathbf{v}_k^T$ and seek an amplification factor $G_{\text{full}}(m, k)$ such that $U^{n+1} = G_{\text{full}}(m, k) U^n$. Substituting this mode into the scheme and using the definition of $Q(U)$ in (4.1) gives:

$$G_{\text{full}}(m, k) \mathbf{x}_m \mathbf{v}_k^T - \theta \frac{\Delta t}{(\Delta x)^2} M_\beta (G_{\text{full}}(m, k) \mathbf{x}_m \mathbf{v}_k^T) A^T = \mathbf{x}_m \mathbf{v}_k^T + (1 - \theta) \frac{\Delta t}{(\Delta x)^2} M_\beta (\mathbf{x}_m \mathbf{v}_k^T) A^T.$$

Using the eigenvector properties, this simplifies to:

$$G_{\text{full}}(m, k) \mathbf{x}_m \mathbf{v}_k^T - \theta G_{\text{full}}(m, k) \frac{\lambda_k \beta_m \Delta t}{(\Delta x)^2} \mathbf{x}_m \mathbf{v}_k^T = \mathbf{x}_m \mathbf{v}_k^T + (1 - \theta) \frac{\lambda_k \beta_m \Delta t}{(\Delta x)^2} \mathbf{x}_m \mathbf{v}_k^T.$$

Comparing both sides and using $\nu_k = \lambda_k \frac{\Delta t}{(\Delta x)^2}$, we have

$$G_{\text{full}}(m, k) = \frac{1 + (1 - \theta) \beta_m \nu_k}{1 - \theta \beta_m \nu_k}.$$

Define $x = -\beta_m \nu_k = 2Y_m \nu_k$. Since $Y_m \in [0, 2]$, $x \in [0, 4\nu_k]$. The amplification factor in terms of x is:

$$G_{\text{full}}(m, k) = \frac{1 - (1 - \theta)x}{1 + \theta x}.$$

For stability, we require $|G_{\text{full}}(m, k)| \leq 1$, which is equivalent to requiring $(1 - (1 - \theta)x)^2 \leq (1 + \theta x)^2$. Expanding the terms and simplifying the expression leads to the inequality:

$$x(1 - 2\theta) \leq 2.$$

If $\theta \in [1/2, 1]$, then $(1 - 2\theta) \leq 0$. The inequality $x(1 - 2\theta) \leq 2$ is always true for any $x \geq 0$. Thus, the scheme is unconditionally stable.

If $\theta \in [0, 1/2)$, then $(1 - 2\theta) > 0$. The inequality requires $x \leq \frac{2}{1-2\theta}$. Hence a sufficient condition is $\nu_k \leq \nu \leq \frac{1}{2(1-2\theta)}$. \square

We now apply the PSI method with Lie-Trotter splitting to the matrix equation (4.1). The procedure is exactly the same as in Subsection 3.1. If the θ -scheme is used in each substep for time integration, we

arrive at the following scheme:

$$\begin{aligned} U^{(1)} &= U^n + \Delta t((1 - \theta)Q(U^n) + \theta Q(U^{(1)}))V^n(V^n)^T \\ &= U^n + \frac{\Delta t}{(\Delta x)^2}((1 - \theta)M_\beta U^n A^T + \theta M_\beta U^{(1)} A^T)V^n(V^n)^T, \end{aligned} \quad (4.3)$$

$$\begin{aligned} U^{(2)} &= U^{(1)} - \Delta t X^{n+1}(X^{n+1})^T((1 - \theta)Q(U^{(1)}) + \theta Q(U^{(2)}))V^n(V^n)^T \\ &= U^{(1)} - \frac{\Delta t}{(\Delta x)^2}X^{n+1}(X^{n+1})^T((1 - \theta)M_\beta U^{(1)} A^T + \theta M_\beta U^{(2)} A^T)V^n(V^n)^T, \end{aligned} \quad (4.4)$$

$$\begin{aligned} U^{n+1} &= U^{(2)} + \Delta t X^{n+1}(X^{n+1})^T((1 - \theta)Q(U^{(2)}) + \theta Q(U^{n+1})) \\ &= U^{(2)} + \frac{\Delta t}{(\Delta x)^2}X^{n+1}(X^{n+1})^T((1 - \theta)M_\beta U^{(2)} A^T + \theta M_\beta U^{n+1} A^T). \end{aligned} \quad (4.5)$$

For the analysis of this combined three-step scheme, we focus on the cases $\theta = 0$ (where the base scheme is forward Euler), $\theta = 1/2$ (Crank-Nicolson), and $\theta = 1$ (backward Euler).

Theorem 4.2 (Stability of the PSI Using the DtP Approach). *The PSI scheme (4.3)-(4.5) for the parabolic system (2.5), derived using the DtP approach with the central finite difference in space and θ -scheme in time, has the following stability properties. For the CFL number $\nu = \lambda_{\max} \frac{\Delta t}{(\Delta x)^2}$, if the time integrator in each substep is*

- Crank-Nicolson: the scheme is unconditionally stable;
- backward Euler: the scheme is conditionally stable, requiring $\nu \leq \frac{\sqrt{5}-1}{8} \approx 0.1545$;
- forward Euler: the scheme is conditionally stable, requiring $\nu \leq \frac{1+\sqrt{5}}{8} \approx 0.4045$.

Proof. We examine the amplification of a single rank-1 mode $\mathbf{x}_m \mathbf{v}_k^T$, where $\mathbf{x}_m \in \mathbb{C}^{N_x}$ is a spatial Fourier mode given by (2.7) and an eigenvector of M_β with eigenvalue β_m ; $\mathbf{v}_k \in \mathbb{R}^{N_v}$ is an eigenvector of A with eigenvalue λ_k . We further assume \mathbf{v}_k is normalized such that $\mathbf{v}_k^T \mathbf{v}_k = 1$.

For the first step (4.3), we assume $U^n = \mathbf{x}_m \mathbf{v}_k^T$ and seek an amplification factor $P_1(m, k)$ such that $U^{(1)} = P_1(m, k)U^n$. Substituting this mode into the scheme gives:

$$\begin{aligned} P_1(m, k)U^n &= U^n + \Delta t((1 - \theta)Q(U^n) + \theta Q(P_1(m, k)U^n))V^n(V^n)^T \\ &= \mathbf{x}_m \mathbf{v}_k^T + \frac{\beta_m \lambda_k \Delta t}{(\Delta x)^2}(1 - \theta + \theta P_1(m, k))\mathbf{x}_m \mathbf{v}_k^T \\ &= (1 + \beta_m \nu_k(1 - \theta + \theta P_1(m, k)))U^n, \end{aligned}$$

where $\nu_k = \lambda_k \frac{\Delta t}{(\Delta x)^2}$. Therefore,

$$P_1(m, k) = 1 + \beta_m \nu_k(1 - \theta + \theta P_1(m, k)),$$

thus,

$$P_1(m, k) = \frac{1 + (1 - \theta)\beta_m \nu_k}{1 - \theta\beta_m \nu_k}.$$

With similar analysis for (4.4) and (4.5), noting the sign change in (4.4), we obtain:

$$U^{(2)} = \frac{1 - (1 - \theta)\beta_m \nu_k}{1 + \theta\beta_m \nu_k}U^{(1)} := P_2(m, k)U^{(1)},$$

and

$$U^{n+1} = \frac{1 + (1 - \theta)\beta_m \nu_k}{1 - \theta\beta_m \nu_k}U^{(2)} = P_1(m, k)U^{(2)}.$$

Therefore,

$$U^{n+1} = P_1(m, k)P_2(m, k)P_1(m, k)U^n.$$

The total amplification factor over one time step for the mode $\mathbf{x}_m \mathbf{v}_k^T$ is:

$$G_{\text{DtP}}(m, k) = P_1(m, k)^2 P_2(m, k) = \left(\frac{1 + (1 - \theta)\beta_m \nu_k}{1 - \theta\beta_m \nu_k} \right)^2 \frac{1 - (1 - \theta)\beta_m \nu_k}{1 + \theta\beta_m \nu_k}.$$

Define $x = -\beta_m \nu_k = 2Y_m \nu_k \in [0, 4\nu_k]$. We have

$$G_{\text{DtP}}(m, k) = \left(\frac{1 - (1 - \theta)x}{1 + \theta x} \right)^2 \frac{1 + (1 - \theta)x}{1 - \theta x} := G(x).$$

Case 1: $\theta = 1/2$. When $\theta = 1/2$, the amplification factor is

$$G(x) = \frac{1 - x/2}{1 + x/2}.$$

This is the amplification factor for the standard Crank-Nicolson scheme. Therefore, the scheme is unconditionally stable.

Case 2: $\theta = 1$. When $\theta = 1$, the amplification factor becomes:

$$G(x) = \left(\frac{1}{1 + x} \right)^2 \frac{1}{1 - x}.$$

We need $|G(x)| \leq 1$. For $0 \leq x \leq 1$, this requires

$$1 \leq (1 + x)^2(1 - x) \iff x^2 + x - 1 \leq 0 \iff x \leq \frac{-1 + \sqrt{5}}{2}.$$

For $x > 1$, this requires

$$1 \leq (1 + x)^2(x - 1) \iff x^3 + x^2 - x - 2 \geq 0 \iff x \geq 1.2056.$$

The second condition is impossible to satisfy for all possible β_m . For the first one, we require

$$\nu \leq \frac{\sqrt{5} - 1}{8}.$$

Case 3: $\theta = 0$. When $\theta = 0$, the amplification factor becomes:

$$G(x) = (1 - x)^2(1 + x).$$

We need $|G(x)| \leq 1$. This requires

$$(1 - x)^2(1 + x) \leq 1 \iff x^2 - x - 1 \leq 0 \iff x \leq \frac{1 + \sqrt{5}}{2}.$$

Therefore, we require

$$\nu \leq \frac{1 + \sqrt{5}}{8}.$$

□

The above analysis shows that Crank-Nicolson yields unconditional stability, while using either forward Euler or backward Euler results in conditional stability. The time step becomes even more restrictive if the problem is super stiff (i.e., when $\lambda_{\max} \gg 1$). To eliminate the stability constraint for the forward/backward Euler, we therefore propose the following hybrid scheme.

Theorem 4.3 (Stability of a Hybrid DtP Scheme). *The PSI scheme (4.3)-(4.5) for the parabolic system (2.5), derived using the DtP approach with the central finite difference in space, backward Euler in the first and third steps (K-step and L-step), and forward Euler in the second step (S-step), is unconditionally stable.*

Proof. Using the same notation as before, the overall amplification factor for this hybrid scheme is:

$$G_{\text{hybrid}}(x) = \left(\frac{1}{1+x} \right)^2 (1+x) = \frac{1}{1+x},$$

which is the amplification factor for the standard backward Euler scheme. Therefore, the scheme is unconditionally stable. \square

Remark 4.1. *If the PSI method is implemented using Strang splitting, the overall amplification factor over Δt step is*

$$G_{\text{Strang}}(x) = P_1(x/2) \cdot P_2(x/2) \cdot P_1(x) \cdot P_2(x/2) \cdot P_1(x/2),$$

where $P_1(x)$ is the amplification factor for the K and L steps, and $P_2(x)$ is the amplification factor for the S step. Since the Crank-Nicolson scheme is second-order accurate in time, it makes more sense to use it in each substep of the above splitting. From the previous discussion, we have

$$P_1(x) = \frac{1-x/2}{1+x/2} \quad \text{and} \quad P_2(x) = \frac{1+x/2}{1-x/2}.$$

Notably, $P_2(x) = 1/P_1(x)$. Substituting this into the formula for G_{Strang} yields

$$G_{\text{Strang}}(x) = P_1(x/2) \cdot \frac{1}{P_1(x/2)} \cdot P_1(x) \cdot \frac{1}{P_1(x/2)} \cdot P_1(x/2) = P_1(x) = \frac{1-x/2}{1+x/2},$$

which is unconditionally stable.

4.2 PtD approach

We finally analyze the stability of the PtD approach for the parabolic equation. To do so, we first apply the low-rank projection/approximation to the parabolic system (2.5), obtaining three equations (the K, S, and L Steps), and then discretize each equation in the x -variable. For each substep, it is natural to still use the central finite difference scheme to discretize the diffusion operator. Since the overall problem is linear, the low-rank projection and the finite difference discretization commute. Therefore, we conclude directly that the stability result established in the previous subsection for the DtP approach applies here *verbatim*. Note that this is very different from the hyperbolic case: when discretizing the resulting equations, the upwind scheme is used in the K-step, while the central finite difference is applied to the S and L steps (see (3.19), (3.20), and (3.21)).

To see the above conclusion, we start from

$$\partial_t \mathbf{u}^T(t, x) = \partial_{xx} \mathbf{u}^T(t, x) A^T, \quad \mathbf{u} \in \mathbb{R}^{N_v},$$

and consider the low-rank approximation

$$\mathbf{u}^T(t, x) = \mathbf{x}^T(t, x) S(t) V(t)^T, \quad \mathbf{x} \in \mathbb{R}^r, \quad S \in \mathbb{R}^{r \times r}, \quad V \in \mathbb{R}^{N_v \times r},$$

where $\langle \mathbf{x} \mathbf{x}^T \rangle_x = I_r$ and $V^T V = I_r$. The projected equations using PSI read:

- K-step: $\mathbf{k}^T(t, x) = \mathbf{x}^T(t, x)S(t)$,

$$\partial_t \mathbf{k}^T(t, x) = \partial_{xx} \mathbf{k}^T(t, x) \tilde{A}^T, \quad \tilde{A} = V^T A V \in \mathbb{R}^{r \times r}.$$

We then discretize in x using the central difference scheme. Let $\mathbf{k}_j(t) = \mathbf{k}(t, x_j)$,

$$\dot{\mathbf{k}}_j^T = \frac{1}{(\Delta x)^2} (\mathbf{k}_{j-1}^T - 2\mathbf{k}_j^T + \mathbf{k}_{j+1}^T) \tilde{A}^T.$$

Defining the matrix $K(t)$ as in the hyperbolic case, this becomes:

$$\dot{K} = \frac{1}{(\Delta x)^2} M_\beta K \tilde{A}^T. \quad (4.6)$$

- S-step:

$$\dot{S} = -\langle \mathbf{x} \partial_{xx} \mathbf{x}^T \rangle_x S \tilde{A}^T.$$

After discretizing in x using central difference, this becomes:

$$\dot{S} = -\frac{1}{(\Delta x)^2} X^T M_\beta X S \tilde{A}^T. \quad (4.7)$$

- L-step: $L(t) = S(t)V(t)^T$,

$$\dot{L} = \langle \mathbf{x} \partial_{xx} \mathbf{x}^T \rangle_x L A^T.$$

After discretizing in x using central difference, this becomes:

$$\dot{L} = \frac{1}{(\Delta x)^2} X^T M_\beta X L A^T. \quad (4.8)$$

Applying the θ -scheme in each of the substeps (4.6), (4.7), and (4.8) results in the following schemes:

$$U^{(1)} = U^n + \frac{\Delta t}{(\Delta x)^2} \left((1 - \theta) M_\beta (U^n V^n) \tilde{A}^T + \theta M_\beta (U^{(1)} V^n) \tilde{A}^T \right) (V^n)^T, \quad (4.9)$$

$$U^{(2)} = U^{(1)} - \frac{\Delta t}{(\Delta x)^2} X^{n+1} \left((1 - \theta) (X^{n+1})^T M_\beta (U^{(1)} V^n) \tilde{A}^T + \theta (X^{n+1})^T M_\beta (U^{(2)} V^n) \tilde{A}^T \right) (V^n)^T, \quad (4.10)$$

$$U^{n+1} = U^{(2)} + \frac{\Delta t}{(\Delta x)^2} X^{n+1} \left((1 - \theta) (X^{n+1})^T M_\beta U^{(2)} A^T + \theta (X^{n+1})^T M_\beta U^{n+1} A^T \right), \quad (4.11)$$

where $\tilde{A} = (V^n)^T A V^n$. (4.11) is identical to (4.5) in the DtP approach. While (4.9) and (4.10) are formally different from (4.3) and (4.4), we find that their action on the rank-1 ansatz $U^n = \mathbf{x}_m \mathbf{v}_k^T$ used in the von Neumann analysis is equivalent. Therefore, the overall amplification factor is the same in both approaches, leading to an identical stability analysis.

5 Conclusion

In this paper, we analyze the stability of the low-rank PSI applied to linear hyperbolic and parabolic equations. The spatial discretization is assumed to be either the upwind finite difference scheme or the central difference scheme. Using a von Neumann-type analysis, we address two questions related to this class of low-rank integrators. 1) For the hyperbolic equation, the stability conditions in the DtP and PtD approaches do not differ when using Lie-Trotter splitting (though both are more restrictive than the full tensor scheme), while the stability region can be much larger when using Strang splitting. 2)

For the parabolic equation, despite the presence of a negative S-step, the method can be unconditionally stable, if Crank–Nicolson or a hybrid forward–backward Euler scheme is used for time stepping, making it suitable for stiff and dissipative problems. While our analysis is limited to simple prototype equations, these equations resemble the structure of many operators arising in kinetic theory. Thus, the results shed light on the behavior of PSI when applied to more complex kinetic problems. Future directions include studying the stability of high-order splitting schemes and high-order temporal and spatial discretizations.

Acknowledgement

This work was partially supported by DOE grant DE-SC0023164, NSF grants DMS-2409858 and IIS-2433957, and DoD MURI grant FA9550-24-1-0254.

References

- [1] G. CERUTI, J. KUSCH, AND C. LUBICH, *A rank-adaptive robust integrator for dynamical low-rank approximation*, BIT Numer. Math., 62 (2022), pp. 1149–1174.
- [2] G. CERUTI, J. KUSCH, AND C. LUBICH, *A parallel rank-adaptive integrator for dynamical low-rank approximation*, SIAM J. Sci. Comput., 46 (2024), pp. B205–B228.
- [3] L. EINKEMMER, J. HU, AND Y. WANG, *An asymptotic-preserving dynamical low-rank method for the multi-scale multi-dimensional linear transport equation*, J. Comput. Phys., 439 (2021), p. 110353.
- [4] L. EINKEMMER, J. HU, AND S. ZHANG, *Asymptotic-preserving dynamical low-rank method for the stiff nonlinear Boltzmann equation*, J. Comput. Phys., 538 (2025), p. 114112.
- [5] L. EINKEMMER, K. KORMANN, J. KUSCH, R. MCCLARREN, AND J.-M. QIU, *A review of low-rank methods for time-dependent kinetic simulations*, arXiv:2412.05912v2.
- [6] L. EINKEMMER AND C. LUBICH, *A low-rank projector-splitting integrator for the Vlasov-Poisson equation*, SIAM J. Sci. Comput., 40 (2018), pp. B1330–B1360.
- [7] S. GOTTLIEB, D. KETCHESON, AND C.-W. SHU, *Strong Stability Preserving Runge-Kutta and Multistep Time Discretizations*, World Scientific, 2011.
- [8] J. KUSCH, L. EINKEMMER, AND G. CERUTI, *On the stability of robust dynamical low-rank approximations for hyperbolic problems*, SIAM J. Sci. Comput., 45 (2023), pp. A1–A24.
- [9] R. J. LEVEQUE, *Finite Difference Methods for Ordinary and Partial Differential Equations*, SIAM, Philadelphia, PA, 2007.
- [10] C. LUBICH AND I. OSELEDETS, *A projector-splitting integrator for dynamical low-rank approximation*, BIT Numer. Math., 54 (2014), pp. 171–188.
- [11] C. VILLANI, *A review of mathematical topics in collisional kinetic theory*, in Handbook of Mathematical Fluid Mechanics, S. Friedlander and D. Serre, eds., vol. I, North-Holland, 2002, pp. 71–305.